NUMERICAL EVALUATION OF TIME INTEGRATION SCHEMES IN A DISTURBED FLOW SIMULATION

Leandro F. de Souza
Instituto de Ciências Matemáticas e de Computação, Departamento de Ciências de Computação e Estatística – USP
Av. Trabalhador São-carlense, 400 - Centro Caixa Postal: 668 - CEP: 13560-970 - São Carlos - SP, Brazil
lefraso@icmc.usp.br

Abstract. *This paper presents various time integration schemes and compare their ability to simulate instability waves in a given flow field. The governing equations for two-dimensional, incompressible flows are derived in vorticity-velocity formulation. Many different time integration schemes are tested: forward Euler, Adams-Bashforth, predictor-corrector and Runge-Kutta. The spatial derivatives are calculated using 6th order compact finite difference schemes. The influence of time step refinement is evaluated. The results show the greatest time step allowed by each time integration scheme that give numerically stable solution, free of spurious oscillations. The CFL numbers and total computing time used by each scheme are compared. The results confirm that Runge-Kutta and multipoint schemes are better suitable for studying this kind of flows.*

Keywords: *Time integration schemes, CFL number, Vorticity-velocity formulation, Hydrodynamic instability, Laminar flow transition.*

1. Introduction

In Computational Fluid Dynamics (CFD) the works dealing with unsteady flows are increasing with the capacity of the computers and memory. In order to perform these kind of simulations the time integration scheme should reproduce correctly the physics of the problem. Many different integration schemes are used in CFD. In Direct Numerical Simulations (DNS) the Runge-Kutta schemes are most used. In Large Eddy Simulations (LES) and Unsteady Reynolds-Averaged Navier-Stokes (URANS) a wide variety of schemes are used.

Fasel (1974) and Bestek (1980), used a implicit scheme in the studies of transitional flows by spatial Direct Numerical Simulation. The choice of this time integration scheme was done because they wanted to use a time step large enough to achieve a time periodic result and these kind of schemes are unconditionally stable, without CFL (Courant-Friedrich-Lewy) constraint (Ferziger and Peric, 1997). The recent works of the same transition group (IAG – University of Stuttgart) adopted a classical 4th order Runge-Kutta scheme (Kloker, 1993; Rist and Fasel, 1995; Bonfigli and Kloker, 1998; Gmelin et al., 1999; Meyer et al., 1999). Although this scheme require the solution of the discretized equations 4 times at each time step, the CFL constraint is smaller than other time integration schemes and it is explicit saving time when compared to an implicit method where it is necessary to solve a system every time step.

Willianson (1980) shows some Runge-Kutta schemes which requires only two storage locations per variable (the same storage required by the forward Euler scheme). These schemes should be used when integrating a very large system of differential equations. A 3rd order low storage Runge-Kutta scheme was tested by Souza (2003), in a CFD simulation of laminar-turbulent transition, but the results showed that the total computing time of this scheme was about the same required by the classical 4th order Runge-Kutta scheme and the last scheme was adopted in his work.

In the present paper various time integration schemes are evaluated for a two-dimensional code. The aim here is on inferring what degree of resolution is needed to capture reliably the instantaneous structure of a disturbed flow. The test case is a disturbance propagation over a boundary flat plate. The time integration schemes evaluated are: forward Euler, Adams-Bashforth, Predictor-Corrector and Runge-Kutta Schemes. The spatial derivatives are calculated using a 6th order compact finite difference scheme (Souza et al., 2005). A damping zone is used near the outflow boundary to avoid reflections (Kloker et al., 1993). The paper is divided as follows: in the next section the formulation used is given; section (3.) shows details of the numerical schemes evaluated for time integration; in Section (4.) the propagation of disturbances with the different time integration schemes are given; the conclusions and final comments are given in section (5.).

2. Formulation

In this study, the governing equations are the incompressible, unsteady Navier-Stokes equations with constant density and viscosity. They consist of the momentum equations for the velocity components (u, v) in the streamwise direction (x) and wall normal direction (y):

$$\frac{\partial u}{\partial t} + u\frac{\partial u}{\partial x} + v\frac{\partial u}{\partial y} = -\frac{\partial p}{\partial x} + \nabla^2 u, \tag{1}$$

$$\frac{\partial v}{\partial t} + u\frac{\partial v}{\partial x} + v\frac{\partial v}{\partial y} = -\frac{\partial p}{\partial y} + \nabla^2 v, \tag{2}$$

and the continuity equation:

$$\frac{\partial u}{\partial x} + \frac{\partial v}{\partial y} = 0, \tag{3}$$

where p is the pressure and

$$\nabla^2 = \frac{1}{Re}\left(\frac{\partial^2}{\partial x^2} + \frac{\partial^2}{\partial y^2}\right). \tag{4}$$

The variables used in the above equations are non-dimensional. They are related to the dimensional variables by:

$$x = \frac{\bar{x}}{\bar{L}}, \quad y = \frac{\bar{y}}{\bar{L}}, \quad u = \frac{\bar{u}}{\bar{U}_\infty}, \quad v = \frac{\bar{v}}{\bar{U}_\infty}, \quad t = \frac{\bar{t}\bar{U}_\infty}{\bar{L}}, \quad Re = \frac{\bar{U}_\infty \bar{L}}{\bar{\nu}},$$

where Re is the Reynolds number, the terms with an over-bar are dimensional terms: $\bar{L}$ is the reference length, $\bar{U}_\infty$ is the free-stream velocity and $\bar{\nu}$ is the kinematic viscosity.

The vorticity here is defined as the negative curl of velocity vector. Knowing that and taking the negative curl of the momentum equations (1) and (2), one can obtain the vorticity transport equation:

$$\frac{\partial \omega_z}{\partial t} = -u\frac{\partial \omega_z}{\partial x} - v\frac{\partial \omega_z}{\partial y} + \nabla^2 \omega_z. \tag{5}$$

Taking the definition of the vorticity and the mass conservation equation, one can obtain a Poisson equation for v velocity component:

$$\frac{\partial^2 v}{\partial x^2} + \frac{\partial^2 v}{\partial y^2} = -\frac{\partial \omega_z}{\partial x}, \tag{6}$$

The governing equations are complemented by the specification of boundary conditions. At the wall no-slip and no penetration conditions are imposed, except at the suction and blowing region where the wall-normal velocity component is specified. At the inflow the velocity and vorticity components are specified based on the Blasius boundary layer solution. At the upper boundary the vorticity disturbances decay exponentially to zero. Finally, at the outflow boundary the second derivative of all dependent variables are set to zero.

3. Numerical Method

The Eqs.(3, 5) and (6) are solved numerically inside the integration domain shown schematically in Fig. 1. The calculation are done on a orthogonal uniform grid, parallel to the wall. The fluid enters the computational domain at $x = x_0$ and exits at the outflow boundary $x = x_{max}$. Disturbances are introduced into the flow field using a suction and blowing function at the wall in a disturbance strip. This region is located between x_1 and x_2. In the region located between x_3 and x_4 a buffer domain technique (Kloker et al., 1993; Souza et al., 2004) was implemented in order to avoid wave reflections at the outflow boundary. In these simulations a Blasius boundary layer is used as the base flow.

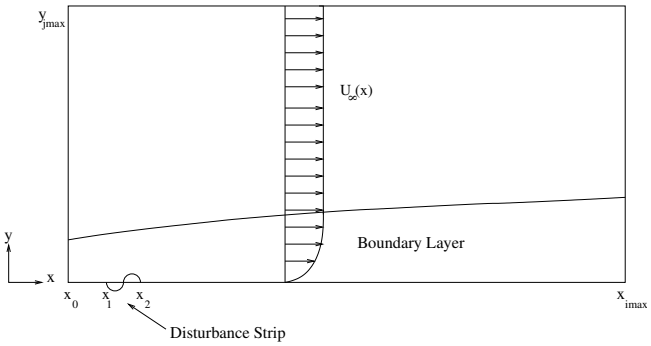

Figure 1. Integration domain.

At the inflow boundary ($x = x_0$), all velocity and vorticity components are specified. At the outflow boundary ($x = x_{max}$), the second derivative of the velocity and vorticity components in the streamwise direction are set to zero. At

the upper boundary ($y = y_{max}$) the flow is assumed to be irrotational. This is satisfied by setting all vorticity and their derivatives to zero. An exponential decay of the velocity is imposed using the condition:

$$\frac{\partial v}{\partial y}|_{x,y_{max},t} = -\beta v(x, y_{max}, t), \tag{7}$$

where β is the disturbance wavenumber.

At the wall ($y = 0$), no-slip condition is imposed for the streamwise (x) velocity component. For the wall-normal velocity component (v) the non-permeability and no-penetration conditions are imposed in all points at the wall except between x_1 and x_2, where the disturbances are introduced. In addition, the condition $\partial v/\partial y = 0$ is imposed to ensure conservation of mass. The equation used for evaluating the vorticity component is:

$$\frac{\partial \omega_z}{\partial x} = -\nabla^2 v. \tag{8}$$

The introduction of the disturbances at the wall is done via a slot in the region ($i_1 \leq i \leq i_2$), where i_1 and i_2 are, respectively, the first and the last point of the disturbance strip, in the x direction. The function used for the variation of the normal velocity v along the streamwise direction is:

$$\begin{aligned} v(i,0,t) = f_1(x) A \sin(\omega_t t + \theta) \qquad & \text{for} \qquad i_1 \leq i \leq i_2 \\ & \text{and} \\ v(x,0,t) = 0 \qquad & \text{for} \qquad i_2 \leq i \quad \text{and} \quad i \leq i_1 \end{aligned} \tag{9}$$

The values of A and θ are real constants that can be chosen to adjust the amplitude and phase of the blowing and suction disturbances. The constant ω_t is the dimensionless frequency. The function $f_1(x)$ adopted was a fifth order function, proposed by Zhang and Fasel (1999). The function is:

$$\begin{aligned} f_1(x) &= \frac{1}{48}(729\epsilon^5 - 1701\epsilon^4 + 972\epsilon^3) \qquad \text{if} \qquad i_1 \leq i \leq \frac{1}{2}(i_1 + i_2) \\ \text{where} \qquad & \epsilon = 2\frac{i - i_1}{i_2 - i_1} \\ \\ f_1(x) &= \frac{-1}{48}(729\epsilon^5 - 1701\epsilon^4 + 972\epsilon^3) \qquad \text{if} \qquad \frac{1}{2}(i_1 + i_2) \leq i \leq i_2 \\ \text{where} \qquad & \epsilon = 2\frac{i_2 - i}{i_2 - i_1} \end{aligned} \tag{10}$$

The chosen function ensures that, at $i = i_1$ and $i = i_2$, the normal velocity component, its first derivatives and second do not have a discontinuity going in and out of the disturbance strip region.

A damping zone near the outflow boundary is defined in which all the disturbances are gradually damped down to zero. This technique is well documented in Kloker et al. (1993), where the advantages and requirements are discussed. In the work of Meitz and Fasel (2000), a fifth order polynomium was adopted and the same function is used in the present simulations. The basic idea is to multiply the vorticity components by a ramp function $f_2(x)$ after each step of the integration scheme. This technique has prove to be very efficient in avoiding reflections that could come from the outflow boundary conditions when simulating disturbed flows. Using this technique, the vorticity components are taken as:

$$\omega_z(x, y) = f_2(x)\Omega_z(x, y, t), \tag{11}$$

where $\omega_z(x, y, t)$ is the disturbance vorticity component that comes out from the Runge-Kutta integration and $f_2(x)$ is a ramp function that goes smoothly from 1 to 0.

The implemented function was:

$$f_2(x) = f(\epsilon) = 1 - 6\epsilon^5 + 15\epsilon^4 - 10\epsilon^3, \tag{12}$$

where $\epsilon = (i - i_3)/(i_4 - i_3)$ for $i_3 \leq i \leq i_4$. The points i_3 and i_4 correspond to the positions x_3 and x_4 in the streamwise direction respectively. To ensure good numerical results a minimum distance between x_3 and x_4 and between x_4 and the end of the domain - x_{max} should be specified. The zones in the simulations presented here has 30 grid points in each region.

The spatial derivatives were calculated using a 6^{th} order compact finite difference scheme (Souza et al., 2005). The v-Poisson equation (6) was solved using a Full Approximation Scheme (FAS) multigrid (Stüben and Trottenberg, 1981). A v-cycle working with 4 grids was implemented.

The numerical procedure works as described below, at each step of the time integration scheme the following instructions are necessary:

1. Compute the Right Hand Side (RHS) of the vorticity transport equation (5);
2. Integrate the vorticity transport equation over one step (or sub-step depending on the scheme);
3. Apply the buffer domain technique near the outflow boundary;
4. Calculate v velocity from the v-Poisson equation (6);
5. Calculate u velocity from the continuity equation (3);
6. Calculate the vorticity generation at the wall using the new v velocity distribution.

The time integration schemes evaluated here are: forward Euler; 2nd, 3rd, 4th and 5th order Adams-Bashforth; 3rd and 4th order Predictor-Corrector and 4th order Runge-Kutta scheme. The details of the tested schemes are given below.

3.1 Forward Euler

This scheme is one of the most used because of its easy implementation and low computer storage demand. It is called explicit forward Euler scheme and is only first order accurate. The scheme is:

$$\omega_z^{t+1} = \omega_z^t + \Delta t f(t, \omega_z^t) + \frac{1}{2}\frac{\partial^2 \omega_z}{\partial t^2}\Delta t + \text{HOT}, \tag{13}$$

where HOT stands for High Order Terms.

This formulation is usually recommended for the integration of the dissipative or friction terms, because no large precision is required in time, as long as the small scale numerical noise are damped (and the scheme is stable). Unfortunately, the forward Euler scheme is not neutral for various problems, in the sense that some quantities such as mass, momentum or energy are not conserved but may decay or grow as the simulation is advanced in time. When these quantities grow with time, the model is of course unstable.

3.2 Adams-Bashforth schemes

The Adams-Bashforth schemes are classified as multipoint schemes and the number of storage required are equal the order that one want to obtain. One can not start to integrate directly applying these schemes because the values of anterior time steps are required. Normally a Runge-Kutta scheme is used to start the time integration, and once the values needed are obtained one can switch to Adams-Bashforth schemes. Four different Adams-Bashforth schemes were evaluated. The formula of each one is given below (see Burden and Faires, 2004):

2nd order Adams-Bashforth

$$\omega_z^{t+1} = \omega_z^t + \frac{\Delta t}{2}\left[3f(t, \omega_z^t) - f(t-1, \omega_z^{t-1})\right] + \frac{5}{12}\frac{\partial^3 \omega_z}{\partial t^3}\Delta t^2 + \text{HOT} \tag{14}$$

3rd order Adams-Bashforth

$$\omega_z^{t+1} = \omega_z^t + \frac{\Delta t}{12}\left[23f(t, \omega_z^t) - 16f(t-1, \omega_z^{t-1}) + 5f(t-2, \omega_z^{t-2})\right] + \frac{3}{8}\frac{\partial^4 \omega_z}{\partial t^4}\Delta t^3 + \text{HOT} \tag{15}$$

4th order Adams-Bashforth

$$\begin{aligned} \omega_z^{t+1} &= \omega_z^t + \frac{\Delta t}{24}[55f(t, \omega_z^t) - 59f(t-1, \omega_z^{t-1}) + \\ &\quad +37f(t-2, \omega_z^{t-2}) - 9f(t-3, \omega_z^{t-3})] + \frac{251}{720}\frac{\partial^5 \omega_z}{\partial t^5}\Delta t^4 + \text{HOT} \end{aligned} \tag{16}$$

5th order Adams-Bashforth

$$\begin{aligned} \omega_z^{t+1} &= \omega_z^t + \frac{\Delta t}{720}[1901f(t, \omega_z^t) - 2774f(t-1, \omega_z^{t-1}) + \\ &\quad +2616f(t-2, \omega_z^{t-2}) - 1274f(t-3, \omega_z^{t-3}) + 251f(t-4, \omega_z^{t-4})] + \frac{95}{288}\frac{\partial^6 \omega_z}{\partial t^6}\Delta t^5 + \text{HOT} \end{aligned} \tag{17}$$

3.3 Predictor-Corrector schemes

The schemes evaluated here are composed by a predictor schemes given by a Adams-Bashforth scheme and a corrector given by a Adams-Moulton scheme. The advantage in using these schemes is that the prediction given by the explicit scheme is corrected by the implicit scheme, thus given a better approximation. Since the schemes needed values of anterior time steps a Runge-Kutta scheme was used to initiate the time integration. Two different predictor-corrector schemes were tested, a third order and a fourth order scheme, the respective formula are given below (see Burden and Faires, 2004):

3rd order Predictor-Corrector

$$\omega_z^{(t+1)^*} = \omega_z^t + \frac{\Delta t}{12}\left[23f(t,\omega_z^t) - 16f(t-1,\omega_z^{t-1}) + 5f(t-2,\omega_z^{t-2})\right] + \frac{3}{8}\frac{\partial^4\omega_z}{\partial t^4}\Delta t^3 + \text{HOT} \tag{18}$$

$$\omega_z^{t+1} = \omega_z^t + \frac{\Delta t}{12}\left[5f(t+1,\omega_z^{(t+1)^*}) + 8f(t,\omega_z^t) - f(t-1,\omega_z^{t-1})\right] + \frac{1}{24}\frac{\partial^4\omega_z}{\partial t^4}\Delta t^3 + \text{HOT} \tag{19}$$

4th order Predictor-Corrector

$$\begin{aligned}\omega_z^{(t+1)^*} &= \omega_z^t + \frac{\Delta t}{24}[55f(t,\omega_z^t) - 59f(t-1,\omega_z^{t-1}) + \\ &\quad +37f(t-2,\omega_z^{t-2}) - 9f(t-3,\omega_z^{t-3})] + \frac{251}{720}\frac{\partial^5\omega_z}{\partial t^5}\Delta t^4 + \text{HOT}\end{aligned} \tag{20}$$

$$\begin{aligned}\omega_z^{t+1} &= \omega_z^t + \frac{\Delta t}{24}[9f(t+1,\omega_z^{(t+1)^*}) + \\ &\quad +19f(t,\omega_z^t) - 5f(t-1,\omega_z^{t-1}) + f(t-2,\omega_z^{t-2})] - \frac{19}{720}\frac{\partial^5\omega_z}{\partial t^5}\Delta t^4 + \text{HOT}\end{aligned} \tag{21}$$

3.4 Runge-Kutta scheme

The difficulties in starting multipoint schemes can be overcome by using points between t and $t+1$ rather than earlier points (Ferziger and Peric, 1997). Schemes of this kind are called Runge-Kutta schemes. The most popular one is of fourth order. The Runge-Kutta schemes of a given order are more accurate (i.e. the coefficient of the error is smaller) and more stable than multipoint schemes of the same order (Ferziger and Peric, 1997). The classical fourth order Runge-Kutta scheme formula is:

$$\begin{aligned}\omega_z^{(t+\frac{1}{2})^*} &= \omega_z^t + \frac{\Delta t}{2}f(t,\omega_z^t),\\ \omega_z^{(t+\frac{1}{2})^{**}} &= \omega_z^t + \frac{\Delta t}{2}f(t+\frac{1}{2},\omega_z^{(t+\frac{1}{2})^*}),\\ \omega_z^{(t+1)^*} &= \omega_z^t + \Delta t\, f(t+\frac{1}{2},\omega_z^{(t+\frac{1}{2})^{**}}),\\ \omega_z^{t+1} &= \omega_z^t + \frac{\Delta t}{6}[f(t,\omega_z^t) + 2f(t+\frac{1}{2},\omega_z^{(t+\frac{1}{2})^*})\\ &\quad +2f(t+\frac{1}{2},\omega_z^{(t+\frac{1}{2})^{**}}) + f(t+1,\omega_z^{(t+1)^*})].\end{aligned} \tag{22}$$

4. Numerical Results

The objective of the numerical simulations in the present study is to verify the greatest time step allowed by the explicit time integration schemes that gives numerically stable solution – without spurious oscillations. Many simulations were carried out and the CFL numbers and the total computing time of each stable solution are shown. In the simulations performed here a very small amplitude disturbance was introduced. The following parameters were used:

$$U_\infty = 30\ \text{m/s},\ L = 5\times10^{-2}\ \text{m},\ \nu = 1.5\times10^{-5}\ \text{m}^2/\text{s},\ \text{and}\ Re = 10^5. \tag{23}$$

The integration domain used for all tests is shown in Fig. (1). It extends from $x_0 = 1.00$ to $x_{max} = 3.88$ in the streamwise direction and from $y_0 = 0.00$ to $y_{max} = 0.08$ in the wall normal direction. The number of points used

was 257 and 81 in the streamwise and wall normal directions respectively. The disturbances were generated between $x_1 = 1.225$ and $x_2 = 1.45$. The dimensionless frequency used was $\omega_t = 10$ and is defined as $\omega_t = (\beta/Re) \times 10^4$. The disturbance amplitude introduced was set to $A = 1 \times 10^{-4}$ and the phase to $\theta = 0$. After 20 time periods, the data were analyzed. These 20 periods corresponds to the introduction of 20 disturbances Tollmien-Schlichting waves in the domain. This test case was already performed in Souza et al. (2002), were a 4^{th} order Runge-Kutta scheme were adopted for time integration. In Souza et al. (2002) the results obtained were compared with Linear Stability Theory (LST) and with a Parabolized Stability Equation (PSE) code, showing a quantitative comparison of the code. Since the verification of the present code was previously done it is not showed here where the focus was the stability of time integration scheme.

For each integration scheme several simulations were carried out. In these simulations the solution obtained with different time steps were verified, starting with a big time step and decreasing until a stable solution was obtained. Figure 2 shows a stable solution obtained by $4th$ order Runge-Kutta scheme. In this figure the iso-contours of spanwise vorticity are shown after the introduction of 20 disturbances Tollmien-Schlichting waves in the domain. In this simulation a CFL number of 1.2988 was used. Figure 3 shows the result using Euler scheme with a CFL number of 0.2793. The result shows the introduction of spurious oscillation in the domain, this oscillations results in a non physical solution.

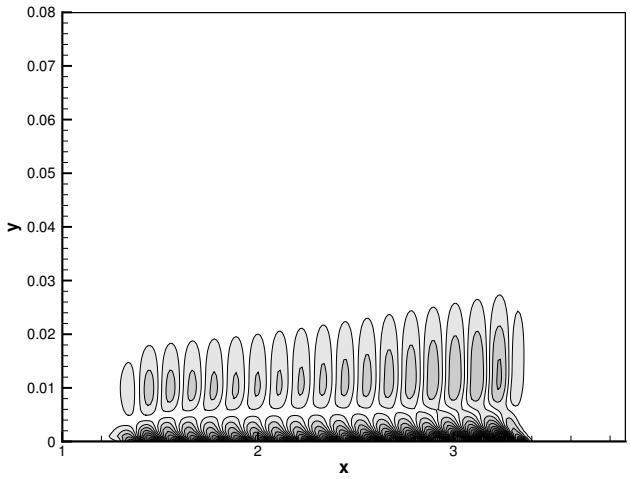

Figure 2. Numerical stable solution, iso-contours of spanwise vorticity.

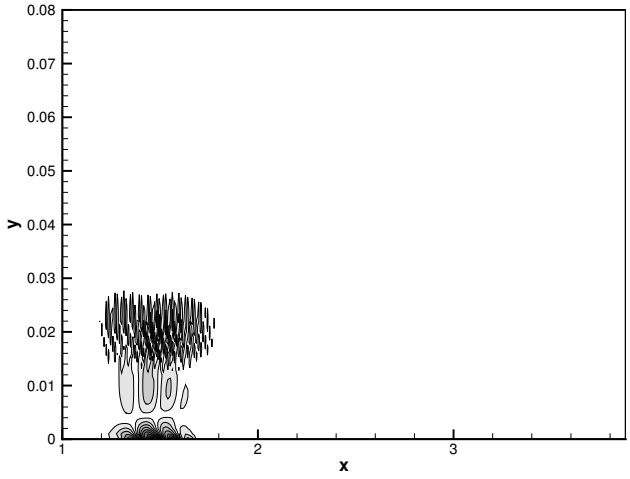

Figure 3. Numerical unstable solution, iso-contours of spanwise vorticity.

All simulations were carried out in a micro computer Pentium IV 2800 MHz. The maximum CFL number that resulted in stable solutions are shown in Table 1. In the same table the total simulation time required by each scheme to solve the problem proposed are shown. This results are also shown in the figures 4 and 5. It can be seen that although the greater CFL number obtained is 1.2988 by the 4th order Runge-Kutta scheme, the total simulation time of the 3rd order Predictor-Corrector method is nearly the same obtained by the Runge-Kutta scheme. This occurs because the 4th order Runge-Kutta scheme requires 4 steps for each integration time step, and the 3rd order Predictor-Corrector scheme uses 2 steps per integration time step.

SCHEME	Runge-Kutta	2nd A-B	3rd A-B	4th A-B	5th A-B	3rd P-C	4th P-C	Euler
CFL	1.2988	0.1802	0.2987	0.1718	0.0922	0.5370	0.4231	0.0114
Simulation time	199.48	550.99	298.36	513.51	937.02	201.17	266.76	6425.32

Table 1. CFL and total simulation time of each numerical scheme.

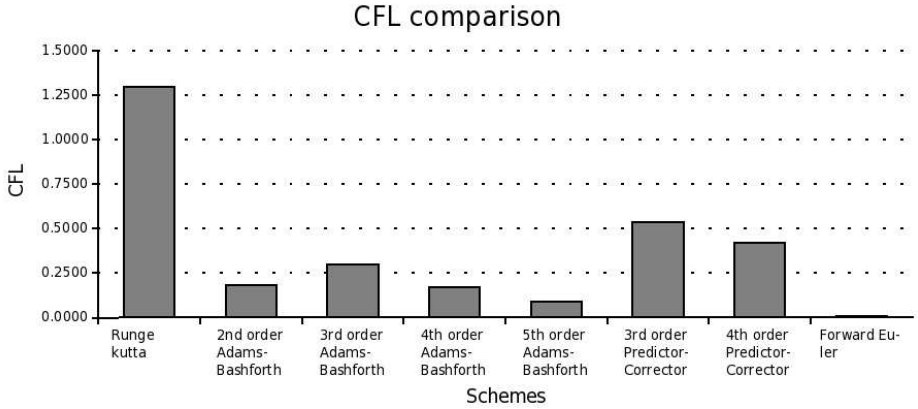

Figure 4. CFL number x Numerical Scheme.

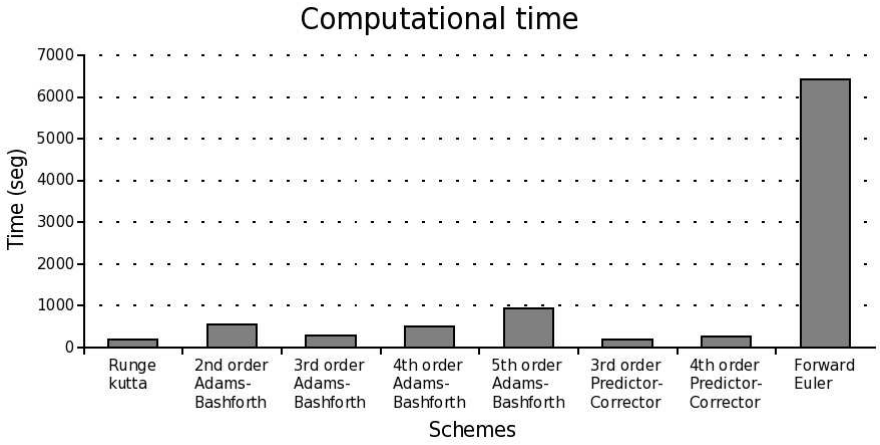

Figure 5. Total simulation time (seg) x Numerical Scheme.

The predictor corrector schemes showed good results. The CFL number of these schemes that resulted in a stable solution were the greater when compared with the other schemes. However this CFL number were lower than the predicted by theory (CFL=1). The Adams-Bashforth schemes achieved good results, ie. did not require a very small CFL number; but only the total simulation time of the 3rd order scheme were attractive. The total simulation time required by the Forward Euler scheme was the greatest among the tested schemes. This was obtained because a stable solution was achieved using a very small CFL number (0.0114).

5. Conclusions

In this paper, the influence of the time integration scheme on the evolution of Tollmien-Schlichting waves was investigated. The simulation using a forward Euler required a very small CFL number to obtain stable solution, turning this scheme economically unfeasible, for this kind of study. The result obtained with this scheme took more then 32 times the simulation time of the greatest CFL number with the 4th order Runge-Kutta scheme.

For the simulations with the Adams-Bashforth schemes, one can observe that the CFL number required was greater then the forward Euler scheme. The total simulation time required by the simulations showed that only the 3rd order scheme is attractive, although it was nearly 50 % more expansive then the 4th order Runge-Kutta scheme.

The total time simulation with the predictor-corrector schemes were better than the the obtained by Adams-Bashforth schemes. These were achieved because the CFL number required by these schemes, to obtain a stable solution, were greater than the ones required by the Adams-Bashforth schemes. The total simulation time required by the 3rd order predictor-corrector scheme was nearly the same obtained by the 4th order Runge-Kutta scheme; and the 4th order predictor-corrector was nearly 25 % more expansive then them.

The results with 4th order Runge-Kutta scheme showed that CFL number up to 1.2988 could be used, turning this scheme the faster to solve the problem proposed.

The main conclusion is that using high order schemes for time integration in DNS studies of laminar-turbulent transition can reduce the total simulation time and these schemes should be used in these kind of studies were a wide range of time scales have to be accurately solved.

6. Acknowledgments

The author acknowledges the support received from FAPESP under grant No 04/07507-4.

7. References

Bestek, H., 1980, "Numerische Untersuchungen zur nichtlinearen räumlichen Störungsanfachung in der ebenen Poisuille-Strömung", PhD thesis, Universität Stuttgart.

Bonfigli, G. and Kloker, M., 1998, Spatial Navier-Stokes Simulation of Crossflow Induced Transition in a Three-Dimensional Boundary Layer, "Proc 11th STAB/DGLR Symposium", Berlin.

Burden, R. L. and Faires, J. D., 2004, "Numerical Analisys", Brooks-Cole Publishing.

Fasel, H., 1974, "Untersuchungen zum Problem des Grenzschichtumschlages durch Numerische Integration der Navier-Stokes-Gleichungen", PhD thesis, Universität Stuttgart.

Ferziger, J. H. and Peric, M., 1997, "Computational Methods for Fluid Dynamics", Springer-Verlag Berlin Heidelberg New York.

Gmelin, C., Rist, U., and Wagner, S., 1999, DNS of Active Control of Disturbance in a Boundary-layer, "The IUTAM 99 Symp. on Laminar-Turbulent Transition", Arisona, USA.

Kloker, M., 1993, "Direkte Numerische Simulation des Laminar-Turbulenten Strömungsumschlages in einer Stark Verzögerten Grenzschicht", PhD thesis, Universität Stuttgart.

Kloker, M., Konzelmann, U., and Fasel, H. F., 1993, Outflow Boundary Conditions for Spatial Navier-Stokes Simulations of Transition Boundary Layers, "AIAA Journal", Vol. **31**, pp. 620–628.

Meitz, H. L. and Fasel, H. F., 2000, A compact-difference scheme for the Navier-Stokes equations in vorticity-velocity formulation., "J. Comp. Phys.", Vol. **157**, pp. 371–403.

Meyer, D., Rist, U., Gaponenko, V., Kachanov, Y., Lian, Q., and Lee, C., 1999, Late-Stage Transition Boundary-Layer Structures. Direct Numerical Simulation and Experiment, "The IUTAM 99 Symp. on Laminar-Turbulent Transition", Arisona, USA.

Rist, U. and Fasel, H. F., 1995, Direct Numerical Simulation of Controlled Transition in a Flat Plate Boundary Layer, "J. Fluid Mech.", Vol. **298**, pp. 211–248.

Souza, L. F., 2003, "Instabilidade Centrífuga e transição para turbulência em Escoamentos Laminares Sobre Superfícies Côncavas", PhD thesis, Instituto Tecnológico de Aeronáutica.

Souza, L. F., Mendonça, M. T., de Medeiros, M. A. F., and Kloker, M., 2002, Analisys of Tollmien-Schlichting waves propagation on a flat plate with a Navier-Stokes solver, "9th brazilian congress on thermal engineering and sciences", Caxambu - MG.

Souza, L. F., Mendonça, M. T., de Medeiros, M. A. F., and Kloker, M., 2004, Seeding of Görtler Vortices Through a Suction and Blowing Strip, "RBCM - Journal of the Brazilian Society of Mechanical Sciences", Vol. XXVI, pp. 269–279.

Souza, L. F., Mendonça, M. T., and Medeiros, M. A. F., 2005, The advantages of using high-order finite differences schemes in laminar-turbulent transition studies, "International Journal for Numerical Methods in Fluids", Vol. **48**, pp. 565–592.

Stüben, K. and Trottenberg, U., 1981, "Nonlinear multigrid methods, the full approximation scheme", chapter 5, pp. 58–71, Lecture Notes in Mathematics. Köln-Porz.

Willianson, J. H., 1980, Low-Storage Runge-Kutta Schemes, "Journal of Computational Physics", Vol. **35**, pp. 48–56.

Zhang, H. and Fasel, H. F., 1999, Spatial Direct Numerical Simulation of Görtler Vortices, "AIAA Fluid Dynamics Conference", Norfolk, USA.

8. Responsibility notice

The author(s) is (are) the only responsible for the printed material included in this paper